OPEN ACCESS
JOURNAL OF ADVANCED DIELECTRICS
Vol. 11, No. 4 (2021) 2150020 (11 pages)

DOI: 10.1142/S2010135X2150020X

Investigation of the effect of *in-situ* grown PPy on low frequency dielectric properties and other properties of PVA–PVP blend film

Sushma Jha*,§, Vaishali Bhavsar*,†, K. P. Sooraj‡, Mukesh Ranjan‡ and Deepti Tripathi*

*Department of Physics, School of Science
Gujarat University, Ahmedabad, Gujarat, India

†Applied Sciences and Humanities Department
SAL College of Engineering, Ahmedabad, Gujarat, India

‡Institute for Plasma Research, Gandhinagar
Gujarat, India

§sushmajha31@gmail.com

Received 10 April 2021; Revised 5 June 2021; Accepted 24 June 2021; Published 3 August 2021

Present study is carried out to understand the effect of conducting polymer, polypyrrole (PPy) on structural, morphological, thermal and dielectric properties of bio-compatible polymer blend film of polyvinyl alcohol (PVA) and polyvinyl pyrrolidone (PVP). The growth of PPy in the matrix of PVA–PVP was analyzed using XRD, FT-IR and SEM studies. The shifting in positions and broadening of XRD diffraction peaks of PVA–PVP-PPy from that of PVA–PVP indicates the structural modification and reduction in the crystallinity of the PVA–PVP due to incorporation of PPy. The SEM studies suggest scattered growth of PPy in PVA–PVP matrix at lower concentration of pyrrole monomer. As the monomer concentration is increased, the uniform and interconnected growth of PPy was observed in SEM micrographs. The TGA thermograms show faster thermal degradation of PVA–PVP- PPy films at lower temperature as compared to PVA–PVP films. The blend films of PVA–PVP- PPy exhibited enhanced values of dielectric constant and ac conductivity as compared to the virgin blend film which are observed to increase with increasing concentration of PPy. The high dielectric constant with high ac conductivity exhibited by PVA–PVP-PPy film suggests its possible application as flexible dielectric material for the development of biosensors, energy storage devices in field of green organic electronics.

Keywords: Polyvinyl alcohol; polyvinyl pyrrolidone; polypyrrole; thermal degradation; dielectric.

1. Introduction

Polymer blends and composites are extensively studied class of materials which exhibit various superior properties that their constituent polymers alone do not exhibit.[1–13] They are thus found large number of applications in the areas of electronics, photonics, aerospace, biotechnology, and biomedical sciences.[1–15] Modifications in the properties of polymer blends depend on degree of compatibility and miscibility of the constituent polymers used in the blends.[1,6–8,10–13] In this context, selection of compatible and miscible polymers for development of new polymeric material is an important aspect.

Amongst different compatible polymers for the preparation of blends and composite, polyvinyl alcohol (PVA) and polyvinyl pyrrolidone (PVP) are widely used in various applications such as biosensors, flexible antennas, nano-dielectrics, energy storage devices, supercapacitors, batteries, EMI shielding, UV absorber, membranes, nerve generation, tissue engineering, targeted drug delivery, scaffold generation, etc.[7–11,13–18] PVA and PVP are eco-friendly, hydrophilic, biodegradable, nontoxic and biocompatible polymers.[1,6,7,11–14] These polymers are water-soluble, possess good mechanical strength and form flexible, transparent films when prepared by solution-cast technique. The hydroxyl (–OH) and carbonyl (C=O) functional groups of PVA and PVP, respectively, are highly sensitive toward various functional additives and nanoparticles which results in the formation of compatible polymer blend and composite material.[1,6–18]

Many of the researchers had investigated the effect of various metal oxides (SnO_2, TiO_2, ZnO, $FeCl_3$, Fe_2O_3,CuO, etc.), nanofillers (SiO_2, Al_2O_3, MWCNT, RGO, GO, $AgNO_3$, MgO, HAP, etc.) and salts (Ammonium Nitrate, $MgCl_2$, $CdCl_2$, Li_2CO_3, CuS, etc.) in PVA–PVP matrix and its effect on structural, morphological, thermal, mechanical, optical and dielectric properties.[1,5–18] Sengwa *et al*. prepared SnO_2 dispersed PVA–PVP nanocomposites films for advanced flexible device technologies.[1] Ramesan *et al*. investigated the effect of CuS nanoparticles on different properties of PVA–PVP

§Corresponding author.

blend and found enhancement in mechanical, dielectric and ac conductivity values of the films.[5] Yassin studied nickel–cadmium (Ni–Cd) doped PVA–PVP nanocomposite film and carried out their mechanical, thermal and dielectric studies. They suggested Ni–Cd-based PVA–PVP films as a potential material for designing batteries.[7] Mohammed *et al*. prepared MgO nanoribbon dispersed PVA–PVP nanocomposites films and found improvement in dc conductivity values on inclusion of MgO nanoribbons.[9]

In recent years, intrinsic conducting polymers (ICPs) have attracted attention of many researchers because of their excellent conductivity, high redox process and optimum performance at room temperature.[19] The new developing field of organic electronics is replacing traditional semiconductors and metals used in electronic devices by conducting polymers and their blends/composites which are now coming into practical applications in different fields like optoelectronic devices, sensor materials, electromagnetic shielding and microwave absorbing materials. The polymer-based materials are ''soft'' which gives them an advantage over their inorganic counterparts by enabling fabrication of flexible, highly conformable, light and thin electronic devices. Among numerous available ICPs, polypyrrole (PPy) has gained popularity owing to some of its attractive properties like thermal stability, nontoxicity and high electrical conductivity (from semi-conducting to metallic range).[2–4] It finds a wide range of applicability in biosensors, gas sensors, conducting wires, micro actuators, anti-electrostatic coatings, solid electrolytic capacitors, electro chromic windows & displays, polymeric batteries, electronic devices and functional membranes.[5,19,20] However, PPy suffers from poor mechanical strength with fragile nature and poor solubility.[3] This can be overcome by incorporating PPy in the insulating matrix of compatible polymer/polymer blends.[2,19,21–24] Karuppasamy and Albrais had developed PPy/Cuo-ZnO nanocomposite-based sensing electrodes and investigated their sensitivity toward oxygen, hydrogen and LPG.[24] Das and Sarkar had prepared ethanol gas sensor from PPy embedded in PVA matrix.[19] Jiang *et al*. prepared methanol gas sensor using PVA-PPy and tested their reproducibility. The studies done so far show that the introduction of conducting polymer (PPy) in the insulating matrix of polymers or polymer blends may enhance their suitability as promising polymeric material for sensors, capacitors, biomedical field and EMI shielding.[19,20,22,24,25] Further, literature review also reveals that most of the studies done are either for PPy embedded in insulating polymer matrix (like PVA, PVC, etc.) or with some oxide fillers. Mostly prepared samples were in the form of pellets or electrodes (where coating is done on some substrate).

In present study, an effort is made to explore the avenues of free standing, lightweight and flexible films of PVA–PVP doped with PPy. Here, PVA–PVP blend films doped with different concentrations of intrinsic conducting polymer, PPy (grown *in-situ*) were prepared. The effect of *in-situ* grown PPy on structural, morphological, thermal, electrical and dielectric properties of PVA–PVP-PPy films was studied in detail. The aim is to design polymer films with tailor made conductivity, mechanical flexibility and dielectric properties which is to be achieved by controlled doping of PPy in PVA–PVP matrix. The films with high dielectric constant and good ac conductivity will probably be useful as flexible dielectric material for the development of biosensors, energy storage devices and other microelectronics applications.

2. Experimental Details

2.1. *Materials*

PVA (Mw = 1, 15,000 gm/mol) and PVP (Mw = 40,000 gm/mol) purchased from Loba Chemicals (India) were used for preparation of host polymer matrix. Pyrrole monomer supplied by SRL Chemicals (India) was used as received and anhydrous $FeCl_3$ purchased from Otto Chemicals (India) was used as oxidant for polymerization of Pyrrole monomer. Double distilled water was taken as solvent for sample preparation.

2.2. *In-situ polymerization of PPy in PVA–PVP blend films*

The PVA–PVP blend films were prepared by solution — cast technique at room temperature with humidity level of 25%. Polymerization of pyrrole monomer was carried out by *in-situ* oxidative polymerization method.[15] PVA and PVP were taken in the ratio of 60:40 (weight ratio) and dissolved in 50 ml of pre-heated double distilled water (DDW). Firstly, the solution containing desired amount of PVA and PVP stirred for 1 h at 70 °C temperature and then stirred for 2–3 h at room temperature until a clear solution was obtained. The oxidant ($FeCl_3$) was dissolved separately in 10 ml of DDW at room temperature. Different concentration (20, 30, 40 and 50 wt% with respect to total polymer weight) of pyrrole monomer were mixed with PVA–PVP solution and stirred for 1 h. After complete dissolution of monomer (Py) in PVA–PVP blend solution, oxidant was slowly added and then the solution was further stirred for 1 h. By now the solution turns black which is an indication of polymerization of pyrrole monomer. Finally, this blended solution of PVA–PVP-PPy was poured in glass petri dish and left to dry at room temperature.

2.3. *Characterizations*

Structural characterizations of the films were carried out using XRD and ATR FT-IR spectroscopy. X-ray diffraction patterns were recorded using Bruker's X-ray Diffractometer (Model: D8 Discover) supplied by GMBH (Germany) with Cu–Kα radiation ($\lambda = 1.540$ Å) in the scattering range of (2θ) 10°–80° with scanning rate of 0.01° s^{-1}. Molecular interaction of the films was analyzed using Fourier transform infrared (FTIR) spectra in Attenuated Total Reflection (ATR) mode

using Bruker's FT-IR (Model: ALPHA I) in the wave number range from 400 cm^{-1} to 4000 cm^{-1}. Morphology of the sample was analyzed using Scanning Electron Microscope (SEM) (Model: Merlin VP Compact) supplied by Carl Zeiss. Differential Scanning Calorimetry (DSC) measurements of the samples were performed on Mettler Toledo TGA/DSC system supported with STARe evaluation software. The DSC thermographs of the samples were taken at a scan rate of 10 °C min^{-1} in the temperature range from 40 °C to 400 °C under the atmosphere of dried nitrogen. Thermogravimetric Analysis (TGA) of the samples was performed on Mettler Toledo TG-DTA system supported with STARe evaluation software. Low frequency dielectric data were obtained using Agilent precision LCR meter E4980A with solid test fixture (Model No: 16451B) having electrode of diameter 0.5 cm. The sample was placed between the parallel electrodes of solid test fixture. The parallel capacitance and parallel resistance were measured in the frequency ranges of 100 Hz to 2 MHz at room temperature. Using the obtained data of parallel capacitance (C_p) and parallel resistance (R_p) from LCR meter, the dielectric constant (ε') and dielectric loss (ε'') were determined. Other parameters like loss tangent, complex electric modulus (M^*) and complex impedance (Z^*) were calculated using complex permittivity data.

3. Results and Discussion

3.1. *Structural study*

3.1.1. *XRD analysis*

The XRD diffractograms of PVA–PVP blend film and PPy doped PVA–PVP composite films are shown in Fig. 1. For PVA–PVP films, the diffraction peak observed at 2θ value of 19.4° and 21° angle is attributed to the semicrystalline nature of the PVA and are in good agreement with the results obtained by other researchers.[1,6,8–10,14,15,20] The hump at 2θ value of 22° and 29° corresponds to the amorphous nature of PVP.[1,5,8,14,26] The broad diffraction peaks of medium intensity observed at 2θ = 31°, 36°, 40°, 41° are due to the combined effect of PVA–PVP blend. Collectively two major humps are observed between the 2θ values of 20° to 80°. First intense hump is seen stretched between 2θ = 19°–22° and other with medium intensity between 2θ = 31°–42°. Presence of these two humps suggests the miscibility of PVP with PVA possessing relatively reduced crystallinity as compared to pure PVA.[5,6,8–11,14,15,18,26]

The XRD diffractogram of PVA–PVP with 20 wt% concentration of PPy exhibited broad humps, one stretched between 2θ = 18°–26° and the second lying between 2θ = 34°–42° which is due to amorphous nature of PPy.[4,19,22] Characteristic peaks of constituent polymers are seen to be overlapped and resulted in the formation of broad humps.[19,20,22] On the other hand, for PVA–PVP with 50 wt% concentration of PPy, the diffraction peak associated with host matrix is seen to be present along with some new peaks at 2θ = 36°, 41°, 47°, 52°.

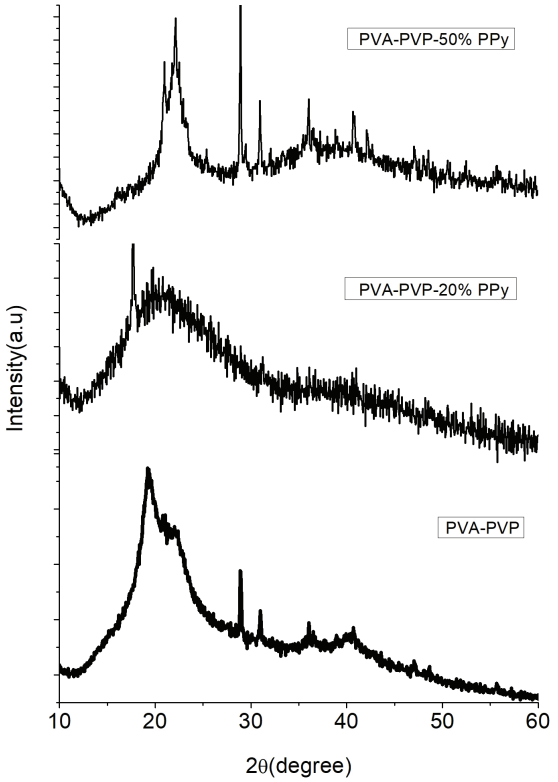

Fig. 1. XRD diffractograms of pure PVA–PVP and PVA–PVP/PPy with 20 wt% and 50 wt% of PPy.

It reveals the fact that inclusion of PPy in PVA–PVP matrix modifies the polymer structure due to interaction between the molecules of PPy and PVA–PVP which result in altered crystallinity of PVA–PVP-PPy blend film.[4,19]

3.1.2. *ATR FT-IR analysis*

The FT-IR spectra of PVA–PVP blend are depicted in Fig. 2(a). The characteristic vibrational peaks of PVA–PVP blend present at 3295 cm^{-1} and 2914 cm^{-1} corresponds to –O-H stretching of PVA and C-H asymmetric stretching vibration of both PVA and PVP chains, respectively.[8,14,15] The peaks present at 1650 cm^{-1}, 1493 cm^{-1} and 1460 cm^{-1} attribute to –C=O stretching of carbonyl group, –C=N (pyridine ring) stretching in PVP and CH bending of CH_2 group present in PVA–PVP blend films, respectively.[8,9,14,15] Peaks positioned at 1438, 1422, 1373 and 1288 cm^{-1} correspond to scissoring, wagging, bending and twisting of CH_2 group present in PVP, respectively.[9,14,15] Vibrational peaks due to C–O stretching of the acetyl group of the blend and C–C stretching of PVA–PVP chains are present at 1090 cm^{-1} and 843 cm^{-1}, respectively.[14,15,13,26] Shifting and broadening of the characteristic peaks of PVA and PVP indicate molecular interaction between the functional group of polymers and miscibility of polymers in the blend film. These observation are in well accordance with literature.[5,8,14,15,23,26]

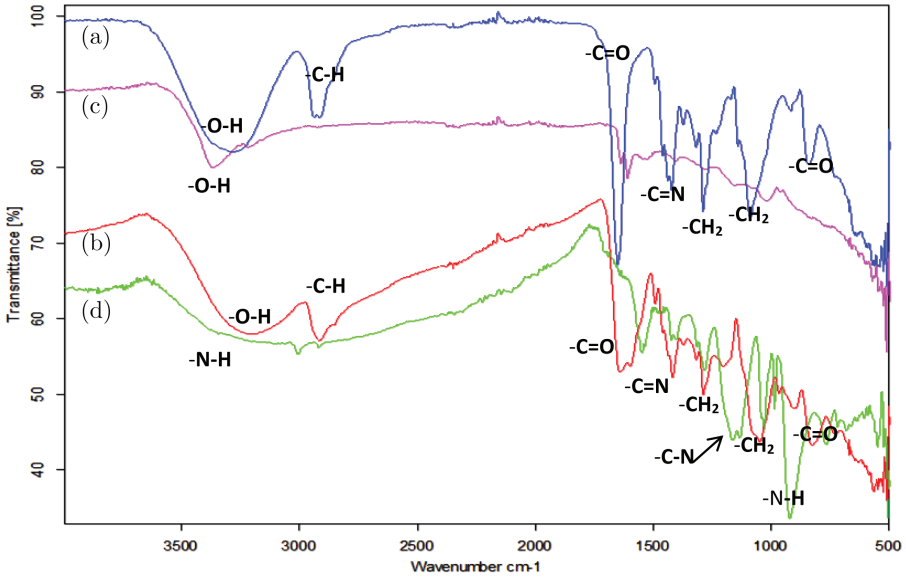

Fig. 2. FT-IR spectra of (a) PVA–PVP blend film, (b) and (c) PVA–PVP with 20 wt% and 50 wt% of PPy blend film and (d) pure PPy.

FT-IR spectra of PVA–PVP-PPy with 20 wt% and 50 wt% weight concentration of PPy are shown in Figs. 2(b) and 2(c), respectively. The vibrational peak associated with N–H stretching of PPy overlapped with O–H stretching vibration of PVA–PVP which undergoes intensity variation and shifts in position. The characteristic peaks seen at 3295 cm^{-1}, 2914 cm^{-1} and 1650 cm^{-1} in PVA–PVP blend are shifted at wavenumber 3198 cm^{-1}, 2915 cm^{-1} & 1642 cm^{-1} and 3371 cm^{-1}, 3218 cm^{-1} & 1638 cm^{-1} in PVA–PVP with 20 wt% PPy and PVA–PVP-50 wt% PPy, respectively. These peaks correspond to the stretching vibration of functional group O–H, C–H and C=O present in PVA–PVP blend, respectively.[14,15,19,20,22] Medium intensity peak at 1492 cm^{-1} is due to the overlapping of –C=C stretching of pyrrole ring and –C=N stretching of pyridine ring in PVP.[14,19] Intense vibrational peak present at wavenumber 1418 cm^{-1} and 1374 cm^{-1} is due to –CH bending.[8,14,19,20] Strong peak at 1287 cm^{-1} and 1286 cm^{-1} is due to CH_2 wagging vibration whereas C–N stretching vibrational peaks are present at 1318 cm^{-1} and 1205 cm^{-1}.[14,26] Peaks at 910 cm^{-1}, 828 cm^{-1} and 733 cm^{-1} correspond to =C–H out of plane deformation, N–H wagging and =C–H wagging vibration, respectively.[22,24]

On increasing PPy concentration (50 wt%) in PVA–PVP matrix, intensity of the characteristic peaks of PPy increases whereas some of the characteristic peaks of PVA–PVP are seen to be overlapped. Peaks at 1704, 1638, 1545, 1409, 1157, 963, 845 and 627 cm^{-1} are some of the characteristic peaks of PPy which undergoes shift and intensity variation on account of increased concentration of PPy.[2,4,19,24,25] The characteristic peaks of constituent polymers in the blend film undergo modification in its width, shapes, positions and intensity after inclusion of PPy that indicate molecular interaction between the constituent polymer and miscibility of PPy with PVA–PVP.[19,20]

3.2. *Morphological study*

3.2.1. *SEM micrograph analysis*

SEM micrograph of PVA–PVP blend is shown in Fig. 3(a). It exhibited a smooth surface due to homogenous mixing of PVA–PVP and good miscibility achieved by strong intermolecular interaction through hydroxyl (O–H) group present in pure PVA and carbonyl (–C=O) group present in PVP.[1,21,27] Threaded structure can be seen at microscopic level on further magnification (enlarged view shown in inset).

SEM micrograph of PPy doped PVA–PVP films are shown in Fig. 3(b). Few granular microstructures of irregular shapes were seen scattered on the surface of PVA–PVP film with 20 wt% concentration of PPy [Fig. 3(b)]. Such granular microstructures were not seen in SEM image of PVA–PVP blend. It suggests the presence PPy on the surface of PVA–PVP. SEM images of this film also exhibited pores indicating irregular growth of PPy in PVA–PVP matrix.[4,19,25] As the weight concentration of PPy increased in PVA–PVP matrix, the granular structure becomes more pronounced and interconnected [Fig. 3(c)]. On comparing these SEM images, it is evident that conducting phase represented by incorporation of PPy network through PVA–PVP matrix depends on the content of pyrrole monomer diffusing within the film during polymerization process. In initial state where the relative PPy content is low as in Fig. 3(b), PPy phase grows discontinuously in PVA–PVP matrix. Increasing concentration of Pyrrole enhances the probability of the formation of interconnecting channels as evident from Fig. 3(c).

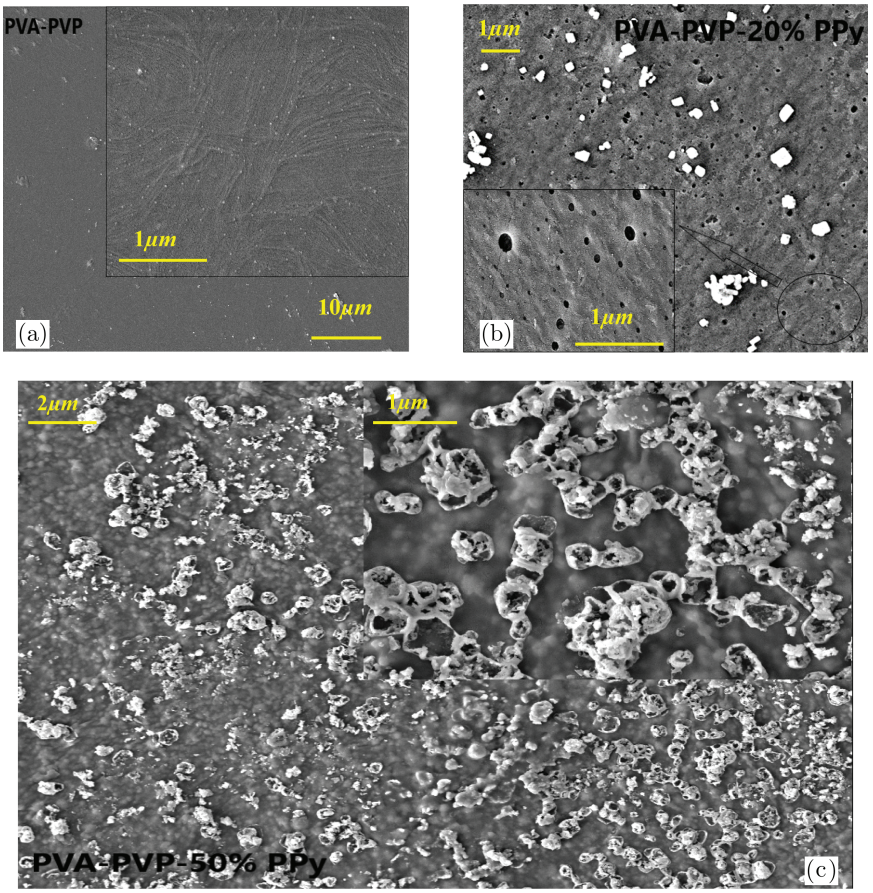

Fig. 3. SEM images of (a) pure PVA–PVP blend film and (b) SEM image of PVA–PVP-20 wt% PPy blend film. Inset shows the enlarged view of circled area. (c) SEM image of PVA–PVP with 50 wt% of PPy. Inset shows the micrographs recorded at higher magnifications.

3.3. *Thermal study*

3.3.1. *Differential scanning calorimetry (DSC) analysis*

The estimation of thermal parameters like glass transition temperature (T_g), melting temperature (T_m), decomposition temperature (T_d) and the associated enthalpies of phase transition gives idea about the microstructural modifications in polymer blends/composites.[14,15,28] DSC thermograms of PVA–PVP blend film and PPy (20 wt% and 50 wt%) doped PVA–PVP blend films are shown in Fig. 4. The values of T_g and T_m for PVA–PVP blend film were observed 64 °C and 197.4 °C which is in good agreement with the literature.[1,23,28] These values are found intermediate of the T_g and T_m values of its constituent polymers (PVA and PVP) as reported by other researcher.[1,5,14,15,23,28] Broad endotherm observed between T_g and T_m is due to micro-Brownian motion of polymer main chain which results in α-relaxation.[1,14,15,28] The enthalpy of phase transition (ΔH) associated with T_g and T_m are 82.85 J/g (ΔH_g) and 8.10 J/g (ΔH_m), respectively for PVA–PVP blend film. For PVA–PVP film with 20 wt% concentration of PPy, value of T_g was 85 °C with associated value of enthalpy change (ΔH_g) is 12.05 J/g. The melting phase temperature T_m can be seen at 200 °C and the associated enthalpy change (ΔH_m) is 16.78 J/g. Film having 50 wt% weight concentration of PPy have T_g at 96 °C (ΔH_g = 131.15 J/g) and T_m (ΔH_m = 29.06 J/g) is nearly at 203 °C. PPy doped PVA–PVP films had exhibited higher T_g and T_m values as compared to host matrix (PVA–PVP). These findings indicate the growth of PPy microstructure in matrix of PVA–PVP which is evidence from SEM micrographs also [Figs. 3(a) and 3(b)]. The increased values of T_g and T_m for PPy doped PVA–PVP blend films are due to complexation of PPy with PVA–PVP that results in the formation of macromolecules which hinder the polymer main chain mobility.[1,3,28] Single glass transition temperature of the blend films suggests appreciable compatibility in its amorphous region and good miscibility of the constituent polymers in the blend films.[1,14,15,23,28] The ΔH_m values were observed increasing for PPy doped PVA–PVP samples and increases with increasing concentration of PPy which suggest stronger molecular interaction between PPy and PVA–PVP.[5]

3.3.2. *TGA analysis*

It is a useful technique to understand thermal decomposition which gives insight into thermal stability of the polymer

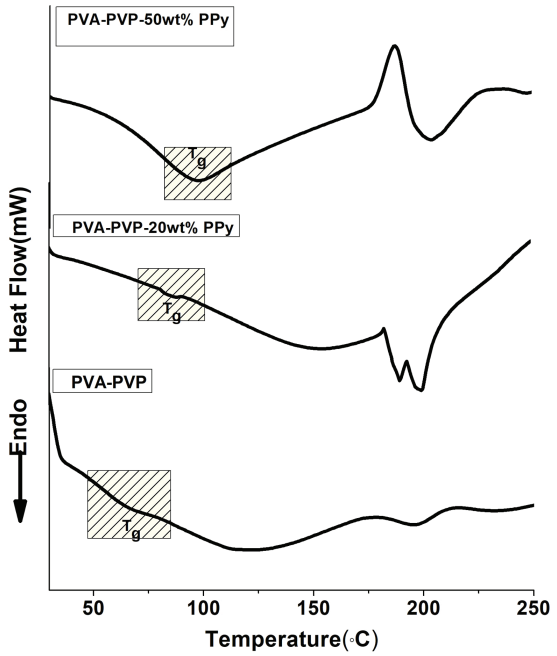

Fig. 4. DSC thermograph of PVA–PVP, PVA–PVP with (20% and 50%) of PPy films recorded under nitrogen atmosphere.

blends and composite materials. It precisely measures the mass loss of the material as a function of temperature in specified atmospheric condition.[2,3,6,25,29] Figure 5 shows the TGA curves of PVA–PVP and PPy (20 wt% and 50 wt%) doped PVA–PVP blend films in the temperature range of 30 °C to 600 °C at heating rate of 10 °C min^{-1}.

PVA–PVP blend doped with 20 wt% concentration of PPy undergoes three stages of thermal decomposition. First stage of decomposition observed in the temperature range of 50 °C to 160 °C with associated mass loss of 19% is due to evaporation of water molecules, unreacted monomer elimination, residual oxidant and oligomers.[30,31] Thermal decomposition

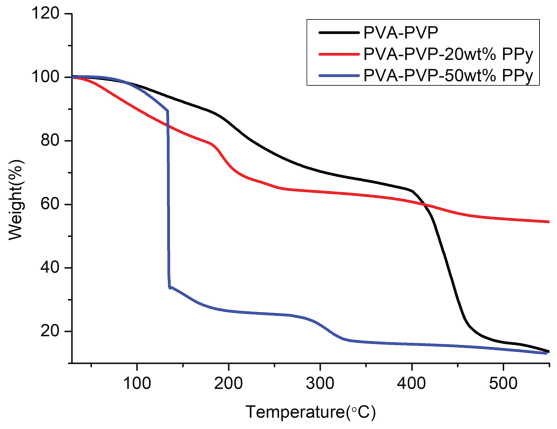

Fig. 5. TGA thermograph of PVA–PVP, PVA–PVP with (20% and 50%) of PPy films recorded under nitrogen atmosphere.

associated with degradation of polymer backbone and loss of C, H and N moieties are observed between the temperature ranges of 160 °C–240 °C with mass loss of 13%.[27,31,32] Final decomposition of polymer residues was observed between 360 °C to 490 °C.[31]

On increasing PPy loading (50 wt%), it decomposes in two stages. First stage decomposition, initiated nearly at 70 °C and ends at 180 °C as a consequence of losing absorbed moisture, residual monomer, unreacted oxidants, low molecular volatile oligomers formed during polymerization process.[28] Maximum weight loss of 69% observed at this stage of decomposition which might be the combined effect of polymer main chain and side chain degradation in association with residual moisture loss.[31,32] Final decomposition stage due to degradation of C–C residues in polymer was observed between the temperature ranges of 370 °C–530 °C.[31]

PPy doped blend films start degrading at lower temperature as compared to PVA–PVP films. This is due to lower thermal degradation of PPy. Also, the interaction of PPy with PVA–PVP weakens the strength of hydrogen bonding between polymeric main chains that lead to thermal degradation of PVA–PVP-PPy blend films at lower temperature.[2,3]

3.4. *Low frequency dielectric study*

3.4.1. *Complex permittivity*

Frequency dependent variation in dielectric constant (ε') and dielectric loss (ε'') for the frequency range of 20 Hz–2 MHz are shown in Figs. 6(a) and 6(b) for PVA–PVP-PPy films. PPy doped samples exhibited higher values of dielectric constant as compared to host matrix and with increasing concentration of PPy, dielectric constant values increase accordingly.

PVA–PVP blend films exhibited insignificant changes in ε' values with varying frequency. The ε' values show slight variation with frequency for lower percentage doping (20 wt% and 30 wt%) of PPy in PVA–PVP matrix. The ε' values of PVA–PVP blend film with 20 wt% of PPy was found in the proximity of host matrix which may be related to scattered growth of PPy and weak interconnecting channels of conducting phase of PPy in PVA–PVP matrix as evident from corresponding SEM image (Fig. 3(b)). However for PVA–PVP blend films with higher concentration of PPy doping, appreciable variation in ε' values was observed with frequency. PVA–PVP blend films with 40 wt% and 50 wt% weight concentration of PPy exhibited pronounced increment in ε' values as compared to undoped PVA–PVP film. The decrease in dielectric constant values with increasing frequency for all polymer blend films is a common behavior exhibited by heterogeneous polymeric material. For PVA–PVP blend films with 40 wt% and 50 wt% weight concentration of PPy, the ε' values were seen to be decreasing sharply with increasing frequency.

Higher values of dielectric constant exhibited by these films at lower frencencies are due to interfacial polarization

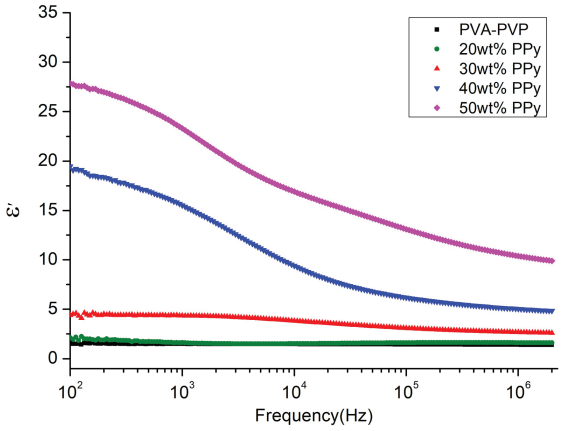

(a)

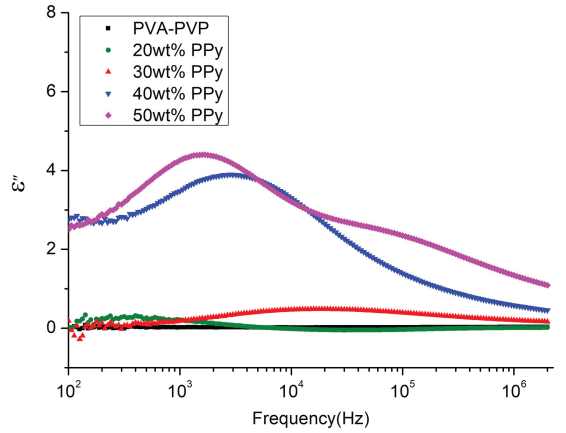

(b)

Fig. 6. (a) and (b) Variation of ε' and ε'' values with frequency from 100 Hz to 2 MHz for pure PVA–PVP and PVA–PVP with PPy (20, 30, 40 and 50 wt%), respectively.

or space charge effect.[14,15] Interfacial polarization originates because of the accumulation of space charges or dipoles at insulator–conductor interface due to slow reversal of applied electric field and in turn dipoles geting enough time to orient themselves.[7,8,14,15] With increasing concentration of PPy (40 wt% and 50 wt%), there is increase in number of dipoles which causes increase in the value of dielectric constant in low frequency region.[31] As the frequency increases, dipoles hardly get enough time to orient themselves with fast varying electric field which results in constant value of ε' at higher frequency.[27] Most of the polarization effect (electrode polarization, interfacial polarization, ionic polarization) takes place in low frequency region or intermediate frequency region.[7,8,14,15,27,31] So, low values of dielectric constant are observed in higher frequency region for polymer blend films under study.

The imaginary part of complex permittivity (ε'') increases first with increase in frequency, thereafter it decreases with increasing frequency for all the blend films [Fig. 6(b)]. The spectra of ε'' for undoped PVA–PVP blend film [Fig. 6(b)] do not show any relaxation peak and show not much change with varying frequency. All PPy doped PVA–PVP films exhibit relaxation peak within experimental frequency range. For PVA–PVP blend film with 20 wt% concentration of PPy, broad relaxation peak can be seen in low frequency region (200 Hz–2 KHz). Enchancement in ε'' values was observed with increasing PPy doping concentration in PVA–PVP matrix. With increase in PPy concentration, these relaxation peaks shift toward intermediate frequency region and become sharper. Relaxation processes in the polymers are consequences of molecular arrangements of the dipoles in dielectric material.[7,27,31] When PPy interacts with hydroxyl and carbonyl groups present in host matrix of PVA–PVP, the cohesive forces acting between macromolecular chains weakens which in turn affect the segmental mobility of polymer main chain. Increased number of dipoles attached to polymer main chain, improves the segmental motion of polymer which corresponds to shift in relaxation peaks to higher frequency side with decreased value of relaxation time.[6,8,14,15,27,31]

3.4.2. *Loss tangent and AC conductivity*

Frequency dependent variation of loss tangent (tan δ) for all the films is shown in Fig. 7(a). The relaxation peaks were found in loss tangent spectra of PPy doped PVA–PVP polymer blend films whereas no relaxation peak was seen for host matrix. The relaxation peaks observed in tan δ spectra of polymer blend films are more intense as that of dielectric loss spectra. With increasing concentration of PPy, tan δ values increase progressively. PVA–PVP blend film having 20 wt% loading of PPy exhibited two relaxation peaks. One peak is in lower frequency region and another relaxation peak gets initiated at 100 kHz frequency which seems to relax beyond the experimental frequency range. PVA–PVP films with 30 wt% and 40 wt% doping of PPy exhibited single relaxation peak in intermediate frequency region (10^3 Hz–10^5 Hz) whereas PVA–PVP having 50 wt% loading of PPy exhibited two relaxation peaks in experimental frequency range. These relaxation peaks are due to combined effects of orientation polarization, electrode polarization and interfacial polarization of the dipoles in polymer blends films.[31,33–34]

Variation in AC conductivity (σ_{ac}) values with frequency for all polymer blend films is shown in Fig. 7(b). The values of σ_{ac} for all films show nonlinear slow rise up to frequency of 10 kHz, thereafter the increase is very sharp in higher frequency region. The undoped PVA–PVP blend film exhibited σ_{ac} values in the range of 10^{-8} S/cm. The ac conductivity values were found to be increasing with the increase of PPy doping in PVA–PVP matrix. PVA–PVP blend film with 30 wt%, 40 wt% and 50 wt% of PPy doping, exhibited systematic rise in σ_{ac} values with increasing concentration of PPy whereas, anomalous behavior was observed for PVA–PVP blend film with 20 wt% doping of PPy. This anomaly in σ_{ac} values at lower percentage (20 wt%) doping of PPy may

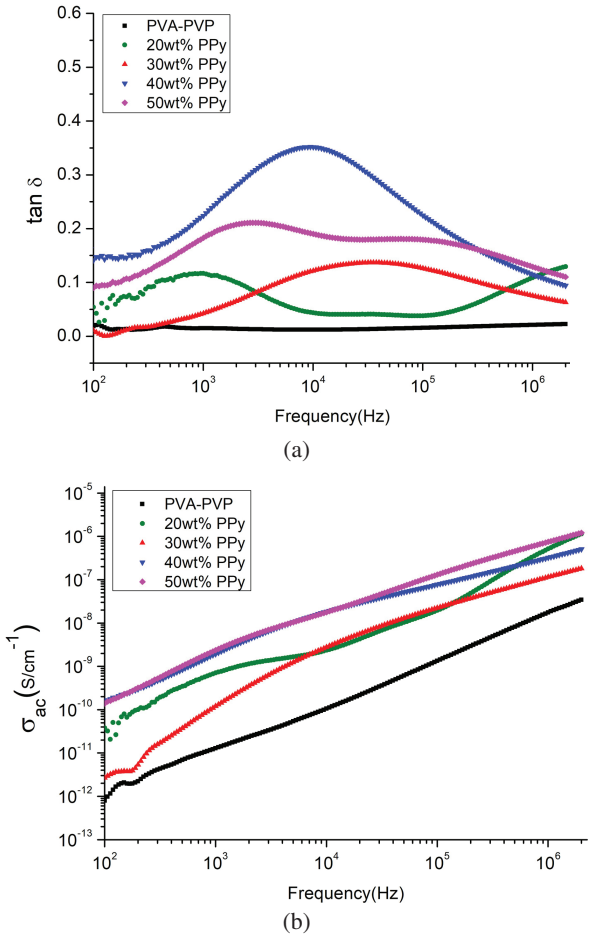

Fig. 7. (a) and (b) Variation of tan δ and σ_{ac} values on log scale with frequency from 100 Hz to 2 MHz for pure PVA–PVP and PVA–PVP doped with PPy (20, 30, 40 and 50 wt%), respectively.

correspond to the inability of PPy to form a continuous conducting path in host matrix as also evident from SEM image [Fig. 3(b)]. On increasing PPy doping concentration, continuous and interconnected conductive channels were formed in the host matrix of PVA–PVP as also seen in its SEM image [Fig. 3(c)] which increases the chain mobility and enhances the σ_{ac} values.[31,33,34]

3.4.3. *Complex electric modulus*

Complex electric modulus formalism separates the contribution of electrode polarization (EP), electrode-dielectric contact and adsorbed impurity effects from bulk properties of the polymeric material.[14] Frequency dependent variations of real (M') and imaginary part (M'') of complex electric modulus are shown in Figs. 8(a) and 8(b). The M' values of all films under study increase gradually with increasing frequency. M' values tend to zero in low frequency region indicating that the dielectric measurements are free from electrode polarization effect.[15,23]

PPy doped PVA–PVP blend films exhibited lower values of M' as compared to undoped PVA–PVP film which decreases with increasing concentration of PPy. A systematic decrease in M' values for PVA–PVP films with 30 wt%, 40 wt% and 50 wt% concentration of PPy was observed whereas some anomaly can be seen in M' values of PVA–PVP with 20 wt% of PPy. The PVA–PVP film with 50 wt% of PPy doping exhibited minimum value of M' and maximum value of dielectric constant which confirms the fact that dielectric constant and real part of electric modulus are reciprocal to each other.[33,34]

M'' spectra [Fig. 8(b)] for all the polymer blend films are in accordance with ε'' and tan δ spectra as the relaxation peaks can be seen in same frequency region. The width of the relaxation peak in M'' spectra increases with reduction in amplitude as compared to ε'' and tan δ spectra. M'' spectra for undoped PVA–PVP film do not exhibit any relaxation. On increasing concentration of PPy in PVA–PVP matrix, relaxation peak shifts to intermediate frequency region which can be attributed to the polymer side chain motion, also known as

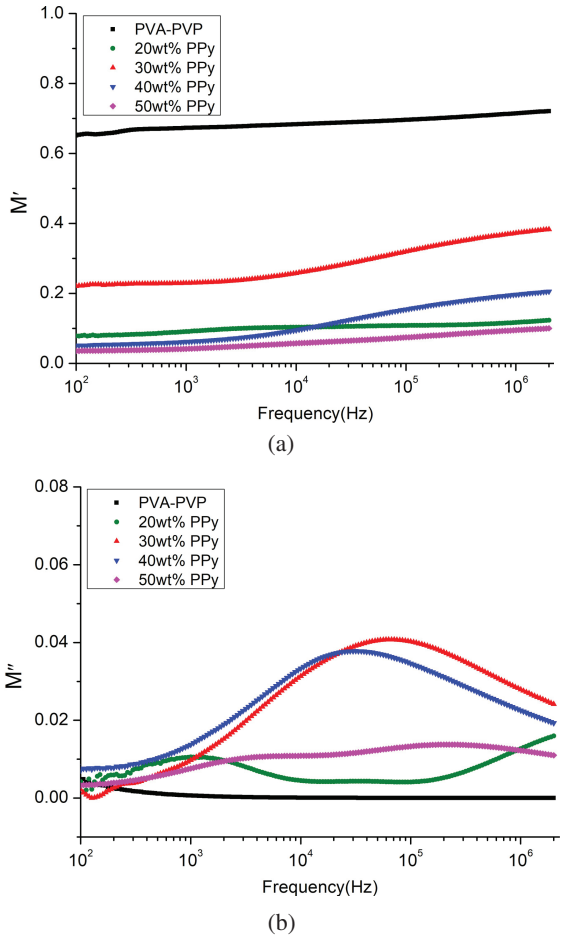

Fig. 8. (a) and (b) Variation of M' and M'' values with frequency from 100 Hz to 2 MHz for pure PVA–PVP and PVA–PVP with PPy (20, 30, 40 and 50 wt%), respectively.

β-relaxation.[14] PVA–PVP blend films with 50 wt% concentration of PPy exhibited two relaxation peaks, one in low frequency region and other in high frequency region. This can be attributed to Maxwell–Wagner–Sillar (MWS) relaxation and coupled effect of relaxation due to side chain motion along with the re-orientation of the functional groups attached to the side chains, respectively.[14,15,17,33,34]

3.4.4. *Complex impedance*

Frequency dependent variation of real part (Z') and imaginary part (Z'') of complex impedance with varying frequency is shown in Figs. 9(a) and 9(b). A linear decrease in Z' values with varying frequency ($f > 1$ kHz) was seen for host matrix which suggest its resistive nature. Whereas, PPy doped PVA–PVP films exhibited nonlinear decrease in Z' values with increasing frequency which may be the contribution of resistive and capacitive element. Z' values of PPy doped PVA–PVP blend films were found higher than the host matrix. Z'' values decrease linearly with increasing frequency for all the polymeric films. Z'' values of PPy doped PVA–PVP films were observed to be less than undoped PVA–PVP film, It decreases with increasing concentration of PPy (30 wt%, 40 wt% and 50 wt%). This observation supports increased value of ac conductivity for PPy doped PVA–PVP films.[31,35]

Complex impedance formalism separates electrode polarization effect and the bulk properties of the material.[23,35] Shape of complex impedance spectra gives us idea about current carriers (electrons or ions) and types of relaxation (Debye or non-Debye). A broad end semi-circle whose center lies on real axis is due to parallel combination of geometrical capacitance and bulk resistance, whereas depressed semicircle in high frequency region with a spike in the low frequency region is the characteristic of diffusion process.[23,36] Depressed semicircle indicates non-Debye type of relaxation and low-frequency spikes indicate the presence of double layer capacitance at the electrode/sample interface.[14,15,35–37]

Complex impedance spectra (Z' versus Z'') of all the polymer blend films are depicted in Fig. 9(c). The shapes of impedance spectra for all the polymer blend films exhibit single arc of a big semi-circle whose center lie below the real axis and these arcs are inclined toward the real axis which

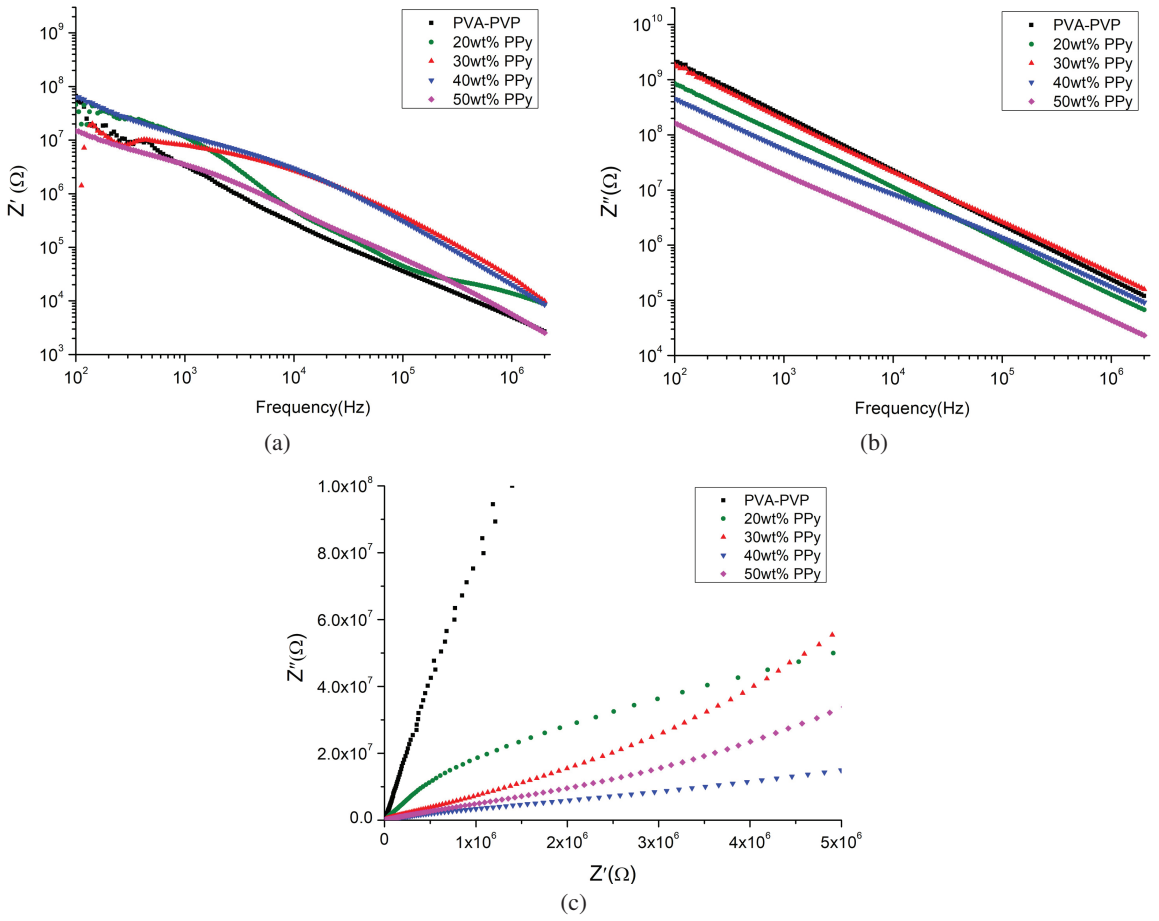

Fig. 9. Variation of (a) Z' values on log scale (b) Z'' values on log scale with frequency for all the blend films and (c) complex impedance spectra.

suggests non-Debye type of relaxation process taking place in all the polymer blend films.[10] This corresponds to bulk properties of the material and that, only electronic conduction exists in these polymeric materials.[35] The complex impedance spectra did not exhibit any spike which indicates good contact of material with electrode and thus eliminating electric double layer (EDL) formation at the electrode.[10,35–37]

4. Conclusion

Polypyrole was grown into PVA–PVP blend films using *in-situ* polymerization and such flexible films are studied for their structural, morphological, thermal and dielectric properties. The XRD difractogram of PVA–PVP blend film confirmed its semi-crystalline nature with reduced intensity than pristine PVA. However, PPy doped PVA–PVP film exhibited lower crystallinity due to uneven and scattered growth of PPy. Growth of PPy in PVA–PVP matrix and molecular interactions of PPy with the chain molecules of PVA–PVP were confirmed by the presence of characteristic FTIR peaks of the constituent polymers. SEM image of PVA–PVP blend film shows smooth surface indicating good miscibility at microscopic level in PVA–PVP blend. The SEM images of PPy doped PVA–PVP films show the presence of some microstructures at surface which indicates the formation of PPy in PVA–PVP matrix. TGA studies indicate better thermal stability of PVA–PVP as compared to PPy doped films. This is due to the disruption of compactness in the structure of PVA–PVP blend by interacting with the grown PPy. PPy doped PVA–PVP blend films exhibited enhanced values of dielectric constant and ac conductivity which was found to increase with increasing concentration of PPy. The high dielectric constant with good ac conductivity exhibited by PPy doped PVA–PVP blend film suggests its possible application as flexible dielectric material for the development of biosensors, energy storage devices and in other microelectronic applications.

Acknowledgments

Authors are thankful to KIRAN Division, Department of Science and Technology (DST), New Delhi for the financial assistance provided through WOS-A project SR/WOS-A/PM-44/2017. Experimental facilities developed using financial assistance provided through DST-FIST (Level-I) and DRS (SAP) program have been utilized to carry out this work and it is gratefully acknowledged. Authors are thankful to Prof. P. N. Gajjar, Head, Department of Physics, School of Science, Gujarat University, Ahmedabad and Prof. V. A. Rana, Department of Physics, School of Science, Gujarat University, Ahmedabad for help extended to take LCR measurements and for his constant encouragement. The extended support of Prof. Rakesh Raval, Department of Biochemistry and Forensic Science, Gujarat University for the utilization of ATR FT-IR facility is also acknowledged.

References

[1]R. J. Sengwa and P. Dhatarwal, Nanofiller concentration-dependent appreciably tailorable and multifunctional properties of (PVP/PVA)/SnO_2 nanocomposites for advanced flexible device technologies, *J. Mater. Sci.: Mater. Electron.* **13**, 1 (2021).

[2]P. Gahlout and V. Choudhary, EMI shielding response of polypyrrole-MWCNT/polyurethane composites, *Synth. Metals* **266**, 116414 (2020).

[3]M. T. Ramesan, K. P. Greeshma, K. Parvathi and T. Anilkumar, Structural, electrical, thermal, and gas sensing properties of new conductive blend nanocomposites based on polypyrrole/phenothiazine/silver-doped zinc oxide, *J. Vinyl Addit. Technol*. **26**, 187 (2020).

[4]V. S. Shanthala, S. N. Shobha Devi and M. V. Murugendrappa, Synthesis, characterization and DC conductivity studies of polypyrrole/copper zinc iron oxide nanocomposites, *J. Asian Ceram. Soc.* **5**, 227 (2017).

[5]M. T. Ramesan, P. Jayakrishnan, T. Anilkumar and G. Mathew, Influence of copper sulphide nanoparticles on the structural, mechanical and dielectric properties of poly (vinyl alcohol)/poly (vinyl pyrrolidone) blend nanocomposites, *J. Mater. Sci.: Mater. Electron.* **29**, 1992 (2018).

[6]M. T. Ramesan, V. K. Athira, P. Jayakrishnan and C. Gopinathan, Preparation, characterization, electrical and antibacterial properties of sericin/poly (vinyl alcohol)/poly (vinyl pyrrolidone) composites, *J. Appl. Polym. Sci.* **133**, 11 (2016).

[7]A. Y. Yassin, Dielectric spectroscopy characterization of relaxation in composite based on (PVA–PVP) blend for nickel–cadmium batteries, *J. Mater. Sci.: Mater. Electron*. **31**, 19447 (2020).

[8]K. Rajesh, V. Crasta, N. B. Rithin Kumar, G. Shetty and P. D. Rekha, Structural, optical, mechanical and dielectric properties of titanium dioxide doped PVA/PVP nanocomposites, *J. Polym. Res.* **26**, 1(2019).

[9]Gh. Mohammed, A. M. El Sayed and W. M. Morsi, Spectroscopic, thermal, and electrical properties of MgO/polyvinyl pyrrolidone/polyvinyl alcohol nanocomposites, *J. Phys. Chem. Solids.* **115**, 238 (2018).

[10]K. Deshmukh, M. B. Ahamed, A. R. Polu, K. K. Sadasivuni, S. K. K. Pasha, D. Ponnamma, M. Al-Ali AlMaadeed, R. R. Deshmukh and K. Chidambaram, Impedance spectroscopy, ionic conductivity and dielectric studies of new Li+ ion conducting polymer blend electrolytes based on biodegradable polymers for solid state battery applications, *J. Mater. Sci.: Mater. Electron.* **27**, 11410 (2016).

[11]N. Rajeswari, S. Selvasekarapandian, C. Sanjeeviraja, J. Kawamura and S. Asath Bahadur, A study on polymer blend electrolyte based on PVA/PVP with proton salt, *Polym. Bull.* **71**, 1061 (2014).

[12]B. Shanthi and S. Muruganand, Structural, vibrational, thermal, and electrical properties of PVA/PVP biodegradable polymer, *Inter J Sci Eng Appl Sci*. **1**, 1105 (2015).

[13]A. S. El-Houssiny, A. A. M. Ward, S. H. Mansour and S. L. Abd-El-Messieh, Biodegradable blends based on polyvinyl pyrrolidone for insulation purposes, *J. Appl. Polym. Sci.* **124**, 3879 (2012).

[14]S. Choudhary and R. J. Sengwa, ZnO nanoparticles dispersed PVA–PVP blend matrix based high performance flexible nanodielectrics for multifunctional microelectronic devices, *Curr. Appl. Phys.* **18**, 1041 (2018).

[15]S. Choudhary, Characterization of amorphous silica nanofiller effect on the structural, morphological, optical, thermal, dielectric and electrical properties of PVA–PVP blend based polymer nanocomposites for their flexible nanodielectric applications, *J. Mater. Sci.: Mater. Electron.* **29**, 10517 (2018).

[16]F. M. Ali and R. M. Kershi, Synthesis and characterization of La 3+ ions incorporated (PVA/PVP) polymer composite films for optoelectronics devices, *J. Mater. Sci.: Mater. Electron.* **31**, 2557 (2020).

[17]G. Kandhol, H. Wadhwa, S. Chand, S. Mahendia and S. Kumar, Study of dielectric relaxation behavior of composites of Poly

(vinyl alchohol) (PVA) and Reduced graphene oxide (RGO), *Vacuum* **160**, 384 (2019).
[18]B. Chaudhuri, B. Mondal, S. K. Ray and S. C. Sarkar, A novel biocompatible conducting polyvinyl alcohol (PVA)-polyvinylpyrrolidone (PVP)-hydroxyapatite (HAP) composite scaffolds for probable biological application, *Colloids Surf. B.* **143**, 71 (2016).
[19]M. Das and D. Sarkar, Development of room temperature ethanol sensor from polypyrrole (PPy) embedded in polyvinyl alcohol (PVA) matrix, *Polym. Bull.* **75**, 3109 (2018).
[20]M. K. Mohanapriya, K. Deshmukh, M. B. Ahamed, K. Chidambaram and S. K. K. Pasha, Influence of cerium oxide (CeO_2) nanoparticles on the structural, morphological, mechanical and dielectric properties of PVA/PPy blend nanocomposites, *Mater. Today: Proc.* **3**, 1864 (2016)
[21]L. Jiang, H.-K. Jun, Y.-S. Hoh, J.-O. Lim, D.-D. Lee and J.-S. Huh, Sensing characteristics of polypyrrole–poly (vinyl alcohol) methanol sensors prepared by in situ vapor state polymerization, *Sens. Actuators B* **105**, 132 (2005).
[22]M. T. Ramesan, In situ synthesis, characterization and conductivity of copper sulphide/polypyrrole/polyvinyl alcohol blend nanocomposites, *Polym.-Plast. Technol. Eng.* **51**, 1223 (2012).
[23]S. Kumar, G. K. Prajapati, A. L. Saroj and P. N. Gupta, Structural, electrical and dielectric studies of nano-composite polymer blend electrolyte films based on (70–x) PVA–x PVP–NaI–SiO_2, *Physica B* **554**, 158 (2019).
[24]H. Albaris and G. Karuppasamy, CuO–ZnO p–n junction enhanced oxygen sensing property of polypyrrole nanocomposite at room temperature, *J. Mater. Sci.: Mater. Electron.* **30**, 9989 (2019).
[25]K. Malook, M. Khan and M. Ali, Polypyrrole-CuO based composites, promotional effects of CuO contents on polypyrrole characteristics, *J. Mater. Sci.: Mater. Electron.* **30**, 3882 (2019).
[26]H. M. Zidan, E. M. Abdelrazek, A. M. Abdelghany and A. E. Tarabiah, Characterization and some physical studies of PVA/PVP filled with MWCNTs, *J. Mater. Res. Technol.* **8**, 904 (2019).
[27]S. Choudhary, Structural, morphological, thermal, dielectric, and electrical properties of alumina nanoparticles filled PVA–PVP blend matrix-based polymer nanocomposites, *Polym. Compos.* **39**, E1788 (2018).
[28]B. M. Baraker and B. Lobo, Multistage thermal decomposition in films of cadmium chloride-doped PVA–PVP polymeric blend, *J. Therm. Anal. Calorim.* **134**, 865 (2018).
[29]M. A. Morsi, M. Abdelaziz, A. H. Oraby and I. Mokhles, Structural, optical, thermal, and dielectric properties of polyethylene oxide/carboxymethyl cellulose blend filled with barium titanate, *J. Phys. Chem. Solids* **125**, 103 (2019).
[30]S. K. Basha, K. Vijay Kumar, G. Sunita Sundari and M. C. Rao, Structural and electrical properties of graphene oxide-doped PVA/PVP blend nanocomposite polymer films, *Adv. Mater. Sci. Eng.* **2018** (2018).
[31]V. Bhavsar and D. Tripathi, Low and high frequency shielding effectiveness of PVC-PPy films, *Polymer Bull. Polym. Bull.* **75**, 2085 (2018).
[32]J. G. Thangamani, K. Deshmukh, K. K. Sadasivuni, D. Ponnamma, K. S. Goutham, V. Rao and S. K. Pasha, White graphene reinforced polypyrrole and poly (vinyl alcohol) blend nanocomposites as chemiresistive sensors for room temperature detection of liquid petroleum gases, *Microchim. Acta*. **184**, 3977 (2017).
[33]R. J. Sengwa, S. Choudhary and P. Dhatarwal, Investigation of alumina nanofiller impact on the structural and dielectric properties of PEO/PMMA blend matrix-based polymer nanocomposites, *Adv. Compos. Hybrid Mater.* **2**, 162 (2019).
[34]B. Chatterjee, N. Kulshrestha and P. N. Gupta, Electrical properties of starch-PVA biodegradable polymer blend, *Phys. Scr.* **90**, 025805 (2015).
[35]V. Bhavsar and D. Tripathi, Surface and dielectric studies of PVC-PVP blend films for green electronics, *Indian J. Pure Appl. Phys.* **56**, 696 (2018).
[36]A. Arya, M. Sadiq and A. L. Sharma, Effect of variation of different nanofillers on structural, electrical, dielectric, and transport properties of blend polymer nanocomposites, *Ionics* **24**, 2295 (2018).
[37]K. Manna, S. K. Srivastava and V. Mittal, Role of enhanced hydrogen bonding of selectively reduced graphite oxide in fabrication of poly (vinyl alcohol) nanocomposites in water as EMI shielding material, *J. Phys. Chem. C* **120**, 17011 (2016).